ISSN 2035-911X

International Journal of
Energy & Technology
www.journal-enertech.eu

International Journal of Energy & Technology 1 (1) (2009) 1–8

CONSTRUCTAL DESIGN OF SOLID STATE FERMENTATION BIOREACTORS

Daniele Colembergue da Cunha[*], Jeferson Avila Souza°, Jorge Alberto V. Costa[*], Luiz Alberto O. Rocha°

[*] School of Chemical and Food, ° School of Engineering
Federal University of Rio Grande, P.O. Box 474, 96201-900, Rio Grande, RS, Brazil.

ABSTRACT

Constructal Design is applied to geometric optimization of an insulated wall bioreactor. The optimization of the bioreactor geometry allows that it to operate, below a certain temperature limit, without external cooling equipment. The possibility of using less equipment shows how geometric optimization can be used as a tool for the ecologically correct management of energy. For the geometric optimization, a mathematical model that represents the solid state fermentation by *Aspergillus niger* is validated and used to study a column fixed bed bioreactor with fixed volume. The model is solved numerically for an insulated wall bioreactor. According to Constructal Design the shape of the bioreactor is free to change subject to volume constraint and in the pursuit of better performance. The optimal ratio between the diameter and the length of the bioreactor, i.e., the ratio which corresponds to the optimal maximum temperature equal to 35 ºC, is calculated for several inlet velocities, volumetric flow rates and inlet air temperatures.

KEYWORDS: *Aspergillus niger*; bioreactor; Constructal Design; heat transfer; optimization; solid-state.

1. INTRODUCTION

Solid state fermentation (SSF) is characterized by the cultivation of microorganisms in a bed of solid particles, free water absence in inter-particle spaces and gas passing through as continuous phase [1 - 3].

From the 90s, SSF has experienced renewed interest due to many potential advantages of this fermentation in comparison with submerged cultivation [4], like smaller bioreactor volumes, reduced downstream processing costs and superior productivity [5 - 8]. However, the major disadvantages are difficulties in monitoring and control of the key process variables at the optimal values for growth and product formation, mainly the temperature and moisture content [4, 9].

Heat arising from metabolic activities of the microorganisms causes a temperature increase in the culture medium [4, 7]. Lack of free water and low conductivity of solid particles can lead to heat gradients in SSF [4]. Although mixing can significantly improve heat removal via the reactor wall, it isn't used in all solid-state reactors, because not all fungi and solid substrates can tolerate the shear and collision forces that result from mixing [4, 9].

In the other side, the difficulty in controlling the temperature in SSF has promoted the necessity of developing new bioreactor configurations or modifying the already existing designs.

The geometric optimization deserved special importance with the appearance of Constructal Theory [10, 11]: "the shape and structure in nature and engineering can be deduced from a principle of global performance maximization subject to global constraints".

A useful tool based on Constructal Theory that can be applied to optimize the bioreactor configuration is Constructal Design: the shape of the biorreactor is free to change subject to volume constraint and in the pursuit of better performance. Constructal Design has been applied successfully to different thermo-fluid systems [12 - 14]. This method proved to be fully versatile and interdisciplinary. For example, it has been extended to hyperthermia cancer treatments: the crucial problem is to keep the temperature of the normal tissue surrounding the tumour below a certain threshold so that the temperature field has to be controlled [15].

The objective of this work is to design a solid-state bioreactor using Constructal Design. A mathematical model to describe the solid-state fermentation by *Aspergillus niger* in a column fixed bed bioreactor was used. The model was solved numerically and validated with experimental data. Then, a bioreactor with insulated wall was optimized for several inlet velocities (v_{in}), volumetric flow rates (Q) and temperatures of inlet air (T_{in}), subject to the volume constraint. The optimal temperature for the growth of *Aspergillus sp*. is 35 ^{o}C [16, 17], therefore this maximum temperature inside the bioreactor was considered the performance indicator.

2. SOLID STATE FERMENTATION

The solid state fermentation considered in this work consisted in the cultivation of *Aspergillus niger* NRRL 3122 in a glass column fixed bed bioreactor, as described by Hasan [18]. The bioreactor was provided by an external heating-cooling jacket to control the temperature. The substrate was the defatted rice bran and rice straw as medium support. Hasan [18] had performed two runs, with monitoring of the

temperature at different points inside the bioreactor (Table 2 indicates the coordinates) by a type J (Copper-Constantine) thermocouple.

3. MATHEMATICAL MODEL AND NUMERICAL METHOD

The mathematical model was proposed for a conventional column fixed bioreactor. The computational domain was defined for the bioreactor of diameter *D* and length *L*, as shown in Fig. 1, in which the saturated air flows through the porous bed and the forced aeration allows enough oxygen supply.

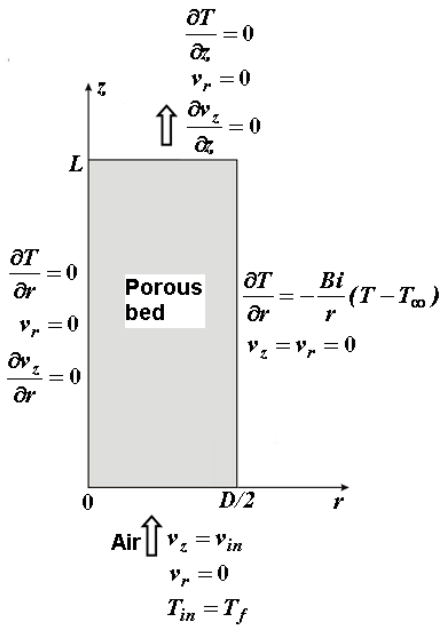

Figure 1. Computational domain and boundary conditions of the bioreactor used for validation of the mathematical model.

The following hypotheses were considered in the mathematical model:

- axisymmetric domain;
- unsteady regime;
- laminar and incompressible flow;
- neglected viscous dissipation;
- constant physical properties (ρ, μ, *Cp*, *k*);
- internal heat generation.

Considering the above assumptions the mass conservation equation can be written as

$$\frac{\partial \rho}{\partial t}+\nabla\cdot(\rho\vec{v})=0 \tag{1}$$

The momentum equation is given by

$$\frac{\partial(\rho_f\vec{v})}{\partial t}+\nabla\cdot(\rho_f\vec{v}\vec{v})=-\nabla p+\nabla\cdot\left(\bar{\bar{\tau}}\right)+\rho\vec{g}-\frac{\mu}{K}\vec{v} \tag{2}$$

where the last term represents the resistance to flow through the porous medium. This term is derived from the relationship between the fluid velocity and pressure gradient expressed by Darcy's law.

The energy equation is given by

$$\frac{\partial(\varepsilon\rho_f e_f+(1-\varepsilon)\rho_s e_s)}{\partial t}+\nabla\cdot[(\vec{v}(\rho_f e_f)]=k_{eff}\nabla^2 T+S \tag{3}$$

where e is the specific total energy (defined by Eq. (4)) and $\vec{v}$ is the surface velocity (see Eq. (5)).

$$e=h-\frac{p}{\rho}+\frac{v^2}{2} \tag{4}$$

$$\vec{v}=(\varepsilon)\vec{v}_{physical} \tag{5}$$

The specific enthalpy, *h*, in Eq. (4) is given by Eqs. (6) and (7), for the solid media and the fluid, respectively.

$$h=\int_{25}^{T} Cp\ dT \tag{6}$$

$$h_f=\int_{25}^{T}(Cp_f+f\lambda)\ dT \tag{7}$$

To calculate the specific enthalpy of fluid (Eq. (7)), the factor $f\lambda$ was added to the term Cp_f. This procedure has been already adopted by several researchers [19-21]. The term $f\lambda$ takes into account that the air remains saturated while flowing through the bed: water evaporation to maintain saturation gives the air larger effective specific heat [22]. It should be noted that Weber et al. [23] did not follow this approach. They verified that there was limitation of the evaporative rate due to hard water mass transfer from the solid to the air. In such cases, it is necessary to include solid-to-gas mass kinetics for the water. Limitation of the evaporative rate was reported for surface velocity equal to 0.011 m s^{-1} for bed composed by oats and 0.021 m s^{-1} for bed composed by hemp [23]. Note that to satisfy the saturated air assumption, two conditions were defined: low temperature gradient within the bioreactor and low inlet air surface velocities (0.003 - 0.006 m s^{-1}).

The energy source term accounts for the volumetric heat generated by the microorganisms, as defined by Eq. (8).

$$S=(1-\varepsilon)\rho_{ds}(-\Delta H)R_{CO2} \tag{8}$$

where R_{CO2} is defined as

$$R_{CO_2}=\frac{d[CO_2]}{dt}=Y_{CO_2}R_s \qquad \text{at } t=0;\ [CO_2]=0 \tag{9}$$

and R_S is given by

$$R_s=-\frac{d[S]}{dt}=\frac{1}{Y_{X/S}}R_X+m[X] \quad \text{at } t=0;\ [S]=[S_0] \tag{10}$$

where

$$R_x=\frac{d[X]}{dt}=\eta_{max}[X]\left(1-\frac{[X]}{[X]_{max}}\right) \tag{11}$$

at $t=0$; $[X]=[X_0]$

and

$$\eta_{max}=\frac{Ae^{[-E_{a1}/R(T+273)]}}{1+B\ e^{[-E_{a2}/R(T+273)]}} \tag{12}$$

The maximum microorganism concentration for *Aspergillus niger* [24] is given by

$$[X]_{max}=0.0000473T^4-0.00403T^3-0.016T^2+7.95T-127.08 \tag{13}$$

The initial conditions are given by

$$t = 0 \qquad T = T_0;\ [X] = [X_0];\ v_z = 0;\ v_r = 0 \tag{14}$$

while the boundary conditions are shown in Fig. 1.

The thermal conductivity of the fermentation medium composed of rice bran (k) was determined using the empirical model [25] (Eq. (15)), which is a function of the packing density of the bed (ρ) and moisture (M).

$$k = 47.5080 + 0.0115\rho + 0.1295M - 6.0737 \ln \rho - 5.5555 \ln M \tag{15}$$

Since the effective thermal conductivity is equal to the weighted average of the void and substrate properties, the thermal conductivity of the solids was obtained by

$$k_s = \frac{k - \varepsilon k_f}{1 - \varepsilon} \tag{16}$$

The domain of Fig. 1 was covered by a mesh with tetrahedral elements using a mesh generation package (Gambit v. 2.3.16 - ANSYS, Inc. - USA). The mesh was exported to the solver package (Fluent v. 6.3.26 - ANSYS, Inc. - USA), where the mathematical model, described by Eqs. (1-16), was solved numerically. The appropriate mesh size was determined by successive refinements, until the further grid doubling of the number of elements met the criterion $\left| (T_{max,\,j} - T_{max,\,j-1}) / T_{max,j} \right| < 0.01$. Here $T_{max,j}$ represents the maximal temperature calculated using the current mesh size, and $T_{max,\,j-1}$ corresponds to the preceding mesh size. Grid independence was achieved using 2500 tetrahedral elements and time step of 600 s.

A statistical methodology was used during the numerical solution validation. The analysis included the correlation coefficients, the maximum temperature error and an analysis of variance (ANOVA) (Table 2). The correlation coefficients were obtained by monitoring the temperature, as a function of time, in selected points inside the experimental bioreactor and comparing them with those determined numerically. The percent error between the numerical and experimental temperature was estimated by

$$Err = 100 \frac{\left| T_{experimental} - T_{simulated} \right|}{T_{experimental}} \tag{17}$$

The analysis of variance used to evaluate the quality of the numerical solution was presented based on F distribution and the significance level (*p-level*) for each temperature point monitored.

The validation of the model was performed by comparing the numerical data of temperature in different positions within the bioreactor with the experimental data obtained by Hasan [18] (two runs named E1 and E2).

The bioprocess E2 was performed using conditions similar to those verified in the E1 bioprocess. However, some parameters presented slight difference: inlet air temperature (29 ºC for E1 and 30 ºC for E2), water temperature at the wall (29.5 ºC for E1 and 30.5 ºC for E2) and initial temperature (26 ºC for E1 and 27 ºC for E2).

The physical properties were assumed constant and their values are shown in Table 1. Additionally, this table specifies the parameters used for the simulations - the references where they were used are also shown.

Figure 2 shows a comparison between experimental results and the numerical solution for temperature profiles in the following bioreactor positions (r, z): (0, 0.25) (a) and (0, 0.30) (b). These bed positions were chosen because of their temperatures are known as the highest inside the bioreactor.

The temperature profiles calculated by the model are consistent with the results given by other authors [18, 21, 28, 29, 32]. There is a maximum temperature due to heat accumulation during the exponential phase of the growth of microorganisms. Note that the model is based on the assumption that the generating heat (Eq. 8) is proportional to the growth of microorganisms according to the logistic equation [33].

Table 1 Parameters and properties used in the simulation.

Constant	Value	Reference
A	7.48 x 10^7 s^{-1}	[24]
B	1.3 x 10^{47}	[24]
Bi[a]	0.8	Estimate value
Cp_f	1 006 J kg^{-1} $ºC^{-1}$	[26]
Cp_s	2 500 J kg^{-1} $ºC^{-1}$	[19, 27, 28]
D	0.047 m	[18, 29]
E_{a1}	70 225 J $gmol^{-1}$	[24]
E_{a2}	283 356 J $gmol^{-1}$	[24]
F	0.00246 kg kg^{-1} $ºC^{-1}$	[19]
K	1.0 x 10^{-8} m^2	[30]
K	0.297 W m^{-1} $ºC^{-1}$	Eq. 15
k_f	0.0242 W m^{-1} $ºC^{-1}$	Fluent database
k_g	0.7 W m^{-1} $ºC^{-1}$	[26]
k_s	0.4139 W m^{-1} $ºC^{-1}$	Eq. 16
L	0.30 m	[18, 29]
M	50 g $(100\ g)^{-1}$	[18, 29]
M	2.0 x 10^{-5} kg kg^{-1} s^{-1}	[24]
R	8.314 J $gmol^{-1}$ K^{-1}	Universal gas constant
v_{in}	0.003 m s^{-1}	[18, 29]
$[X_0]$	0.012 g $(100\ g)^{-1}$	Estimate value
Y_{CO2}	0.29 kg kg^{-1}	[24]
$Y_{X/S}$	0.55 kg kg^{-1}	[24]
ΔH	8.86 J g^{-1}	[31]
E	0.30	[18, 29]
Λ	2 414 300 J kg^{-1}	[19]
μ_f	1.84 x 10^{-5} kg m^{-1} s^{-1}	[26]
P	600 kg m^{-3}	[18, 29]
ρ_{ds}	713.27 kg m^{-3}	Estimate value
ρ_f	1.181 kg m^{-3}	[26]
ρ_s	856.64 kg m^{-3}	Estimate value

[a] Biot number used to agree with [18, 29]

Table 2 shows statistical correlations for both runs E1 and E2 for several positions over time within the bioreactor. It presents, except for one position, correlation coefficients greater than 0.88. Similar results were obtained by Hasan [18]. The model error, that is, the difference between experimental and simulated maximum temperatures, was calculated for different positions in the bioreactor. Table 2 shows a good match - results agree within 8.8 %.

Table 2 also shows the analysis of variance (ANOVA) between the experimental and numerical temperatures at different positions inside the bioreactor, during the entire cultivation entailed process. The numerical model presented in this work is predictive and significant at significance level of 5 %, once the *F* values were very higher than the *F* value of table (*F* table = 4.28) [34]. The low values of significance level (*p-level*) also indicate the good adjustment of the proposed model to the experimental data.

The numerical model was able to predict the bioprocess time when the maximum temperature was reached for both runs E1 and E2. The experimental data E1 presented peak temperature between 34.5 and 39 h of cultivation, similar to the time of 37 h predicted by the numerical model. The experiment E2 presented the peak temperature between 34 and 38.5 h of bioprocess while the numerical model indicated 34 h.

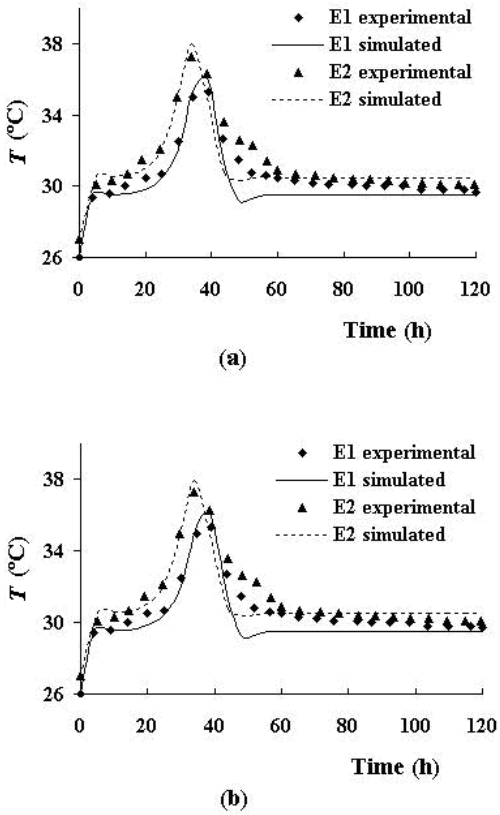

Figure 2. Temperature profiles as function of time at the positions (0, 0.25) (a) and (0, 0.30) (b) during the cultivations.

Figure 3 illustrates the numerically-obtained temperature fields for several times of runs E1 (Fig. 3 (a-c)) and E2 (Fig. 3 (d-f)). These figures show the effect of heat transfer through the wall, producing the parabolic shape in the temperature profiles.

4. THE WALL INSULATED BIOREACTOR

Considering now the bioreactor without the external heating-cooling jacket. If the same geometry, materials and operation conditions are used in the fermentation, the maximum temperature in the bed will be larger than the maximum temperature in the cooled bioreactor, and the process may collapse. However, if the parameter *(D/L)* receives an appropriate value, the aeration could cool the bed adequately without the use external cooling equipment, like cooling jacket. The maximum temperature that maintains the system working properly is considerate 35 ºC.

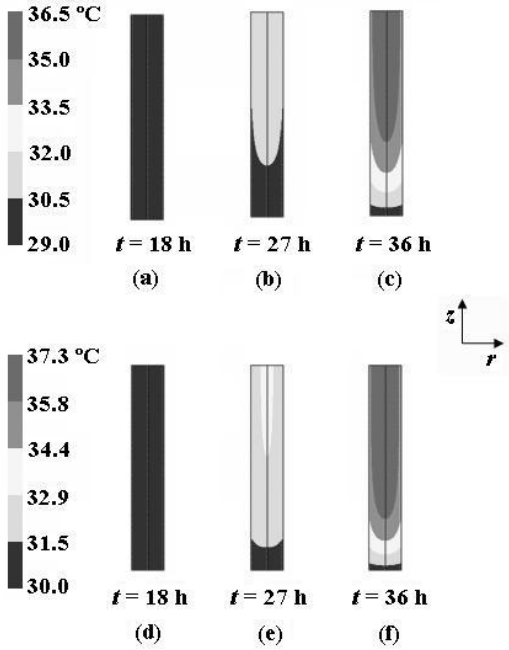

Figure 3. Temperature profiles of runs E1 (a-c) and E2 (d-f) for several times.

The idea to propose bioreactors with insulated walls is not new [20, 21]. The cooling of the substrate bed can be performed by manipulating air flow rate (or inlet velocity) and/or using dynamic changes of air (including air pressure pulsation and air reversal circulation). It is worth to mention that both cooling solutions must be used carefully because, at certain levels, they could affect the growth of the microorganism or the production or the stability of the metabolite.

The performance indicator defined by this work is similar to the one used by Mitchell [20] and Ashley [21]. These researchers assumed that it is undesirable for any part of the bioreactor to reach 5 ºC above the optimum temperature for growth. They referred to this temperature as the critical temperature for growth. According to these authors, in actual fermentation, the critical temperature might correspond to a temperature which triggers sporulation, or which has adverse effects on product formation.

The geometric optimization was performed according to Constructal Design methodology. It was used the same mathematical model and physical properties that were used for the bioreactor with cooling jacket, except for a new boundary condition on the insulated wall that was

$$\text{at } r = R,\ \frac{\partial T}{\partial r} = 0\ ;\ v_z = 0;\ v_r = 0 \tag{18}$$

Table 2. Position, coordinates, correlation coefficient, percent error calculated between experimental and numerical maximal temperatures and analysis of variance between monitored temperatures during the entire cultivation process.

Position	Coordinates (r,z)	Correlation Coefficient		Percent Error		*F*		*p-level*	
		E1	E2	E1	E2	E1	E2	E1	E2
1	(0, 0.05)	0.7841	0.8855	8.2 %	8.8 %	36.727	83.551	0.000004	< 0.000001
2	(0, 0.10)	0.9453	0.8835	6.4 %	6.7 %	193.036	81.846	< 0.000001	< 0.000001
3	(0, 0.15)	0.9600	0.9049	2.9 %	0.3 %	270.086	103.906	< 0.000001	< 0.000001
4	(0, 0.20)	0.9532	0.9155	1.1 %	2.6 %	228.477	119.168	< 0.000001	< 0.000001
5	(0, 0.25)	0.9528	0.9128	3.4 %	1.3 %	226.391	114.949	< 0.000001	< 0.000001
6	(0, 0.30)	0.9324	0.8958	8.0 %	5.9 %	153.094	93.428	< 0.000001	< 0.000001
7	(0.008, 0.15)	0.9794	0.9028	3.5 %	3.1 %	540.675	101.342	< 0.000001	< 0.000001
8	(0.016, 0.15)	0.9700	0.8776	4.5 %	4.0 %	365.959	77.045	< 0.000001	< 0.000001
9	(0.0235, 0.15)	0.9049	0.8841	4.3 %	5.0 %	103.975	82.331	< 0.000001	< 0.000001

The initial temperature was set to 29.5 ºC for all the simulations.

According to the Constructal method the bioreactor volume is a global constraint

$$V = \frac{\pi D^2 L}{4} \tag{19}$$

and it was set to 0.52 x 10^{-3} m^3, which is the volume of the available bioreactors in our laboratory.

The performance indicator is the maximum temperature which must not exceed the optimal temperature for the growth of *Aspergillus sp.* (35 ºC) [16, 17]. The optimization procedure was the following: maintain the volume constant, vary the ratio *(D/L)* to calculate the geometry of the bioreactor and solve the numerical model to obtain the maximum temperature, independent where it is located in the bioreactor. This procedure was repeated for several configurations to obtain the optimal ratio $(D/L)_{opt}$ which corresponds to the minimized maximum temperature, $T_{max,m}$ = 35 ºC.

An example of how the temperature field evolves in time in an insulated bioreactor can be seen in Fig. 4 (a), (b), and (c). This figure shows the temperature field of bioreactor for several time steps (v_{in} = 0.006 m s^{-1}, T_{in} = 29.5 ºC and *(D/L)* = 1). The temperature profile presented an axial temperature gradient, but the radial temperature gradient was negligible (perfect isolation). Therefore, the bed cooling took place due to convective and evaporative heat transfer.

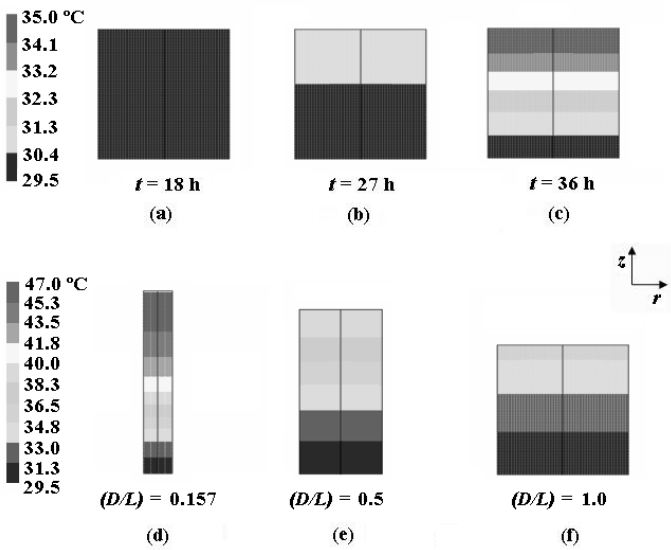

Figure 4. Temperature profiles of the wall insulated bioreactor with optimized geometry at several times (a-c) and temperature profile of 3 different ratios *(D/L)* of the bioreactor (d-f).

Figure 4 (d), (e) and (f), in the other side, illustrates the important role that the ratio *(D/L)* plays on the maximum temperature of the bioreactor. This figure shows the temperature distribution for several ratios *(D/L)* (v_{in} = 0.006 m s^{-1}, T_{in} = 29.5 ºC), including the optimal ratio $(D/L)_{opt}$ = 1 (t = 36 h) according to our optimization criterion.

Figure 5 shows the behavior of the maximum temperature of the bioreactor as function of geometry *(D/L)* when the inlet air temperature, T_{in}, was set equal to 29.5 ºC. This figure (Fig. 5) shows that when the same T_{in} is used the maximum temperature decreases when the ratio *(D/L)* increases. This was expected because, if the inlet velocity is kept constant, the increase of diameter will increase the flow rate in the bioreactor.

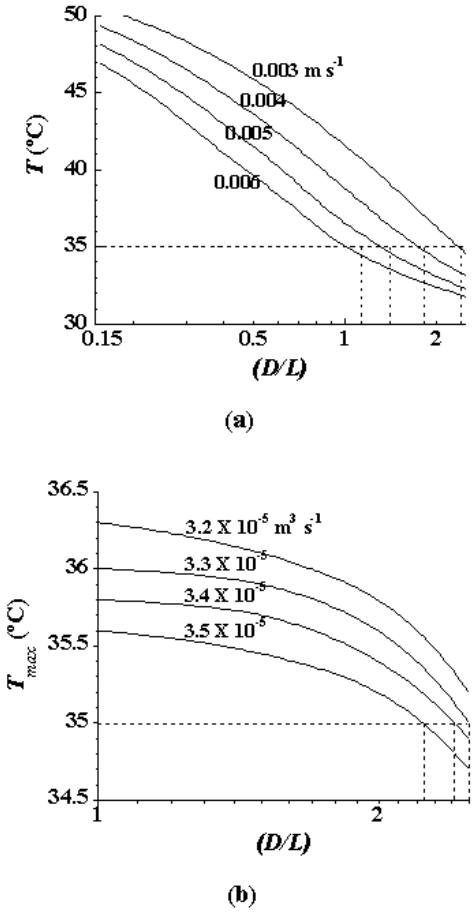

Figure 5. Optimization of the ratio *(D/L)* of the insulated wall bioreactor for several inlet velocities (a) and volumetric flow rates (b).

It was also observed that, if the ratio *(D/L)* is fixed, the maximum temperature decreases when the inlet velocity increases because this will also increase the volumetric flow rate. The optimal ratio $(D/L)_{opt}$, i.e., the ratio which corresponds to the optimal maximum temperature equal to 35 ºC, is shown in Fig. 5 (a) for several inlet velocities (v_{in}). The velocities interval (0.003 - 0.006 m s^{-1}) was previously tested successfully in bioprocesses with the *Aspergillus* fungus using the same bed of substrate [35].

The procedure used in Fig. 5 (a) was repeated in Fig. 5 (b), but now for several volumetric flow rates. Again, as it was expected, the maximum temperature decreases when the volumetric flow rate increases. The optimal maximum temperatures occurred in the range 36-38 h of fermentation for all the simulations shown in Fig. 5.

The effect of the inlet air temperature on the geometric optimization of the bioreactor is shown in Fig. 6. The results indicate that lower inlet air temperatures allow the use of smaller volumetric flow rates in the bioreactor cooling. However, Mitchell et al. [19] do not advise it, because in spite of lower inlet air temperatures decrease the maximum temperature within the bioreactor, there are practical limits on how low T_{in} can be set: it must be sufficiently high to support reasonable specific growth rates, since the entrance region will be maintained around T_{in} by the incoming air.

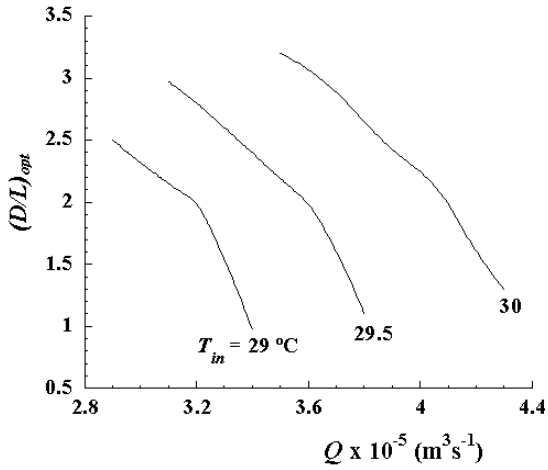

Figure 6. $(D/L)_{opt}$ of the insulated bioreactor as function of the temperature of inlet air.

5. CONCLUSION

This paper uses a mathematical model to describe the solid-state fermentation by *Aspergillus niger* in a column fixed bed bioreactor. The model was solved numerically and validated with experimental data.

The methodology Constructal design was used to optimize the geometry of an insulated wall bioreactor. The geometric optimization of the bioreactor allows that it operates, below a certain temperature limit, without external cooling equipment. The possibility of using less equipment shows how geometric optimization can be used as a tool for the ecologically correct management of energy.

The maximum temperature of the insulated wall bioreactor was analyzed as function of its geometry (ratio (D/L)). When the same T_{in} is used, the maximum temperature decreases when the ratio *(D/L)* increases. This fact happens because, if the inlet velocity is kept constant, the increase of diameter will increase the flow rate in the bioreactor. This observation was confirmed when the volumetric flow rate was kept constant and varied the ratio *(D/L)*.

The effect of the inlet air temperature on the geometric optimization of the bioreactor was also verified. The results indicated that lower inlet air temperatures allow the use of smaller volumetric flow rates in the bioreactor cooling.

It was concluded that the geometry is an important parameter and its optimization can benefit the performance of the bioreactor.

6. NOMENCLATURE

A	frequency factor, s^{-1}
B	dimensionless factor, dimensionless
Bi	wall Biot number [hD/2k], dimensionless
$[CO_2]$	CO_2 concentration, g (100 g dry matter)$^{-1}$
Cp	specific heat, J kg^{-1} $ºC^{-1}$
D	bioreactor diameter, m
e	specific total energy, J kg^{-1}
E_{a1}	activation energy, J $gmol^{-1}$
E_{a2}	inactivation energy, J $gmol^{-1}$
Err	percent error, %
F	statistical F distribution (dimensionless)
f	carrying water capacity, kg water (kg air)$^{-1}$ $ºC^{-1}$
$\vec{g}$	gravity vector, m s^{-2}

h specific enthalpy, J kg^{-1}
h heat transfer coefficient, W m^{-2} $^oC^{-1}$
K bed permeability, m^2
k bed thermal conductivity, W m^{-1} $^oC^{-1}$
L bioreactor length, m
M bed moisture, g (100 g fermented media)$^{-1}$
m cell maintenance coefficient, kg substrate (kg biomass)$^{-1}$ s^{-1}
p static pressure, Pa
p-level significance level, dimensionless
Q volumetric flow rate, m^3 s^{-1}
r radial coordinate, m
R universal constant of gases, J $gmol^{-1}$ K^{-1}
R_{CO2} CO_2 reaction rate, g (100 g dry matter)$^{-1}$ s^{-1}
R_s substrate consumption reaction rate, g (100 g dry matter)$^{-1}$ s^{-1}
R_x microorganism growth rate, g (100 g dry matter)$^{-1}$ s^{-1}
S energy source term, W m^{-3}
$[S]$ substrate concentration, g (100 g dry matter)$^{-1}$
t time, s or h
T temperature, ^oC
V volume, m^3
$\vec{v}$ superficial velocity, m s^{-1}
[X] microorganism concentration, g (100 g dry matter)$^{-1}$
Y_{CO2} substrate-CO_2 yield, kg CO_2 (kg substrate)$^{-1}$
$Y_{X/S}$ substrate-biomass yield, kg biomass (kg substrate)$^{-1}$
z axial coordinate, m

Greek letters

$\bar{\tau}$ stress tensor, Pa
ΔH CO_2 formation heat, J g^{-1}
ε bed porosity, dimensionless
η specific growth rate, s^{-1}
λ vaporization enthalpy, J kg^{-1}
μ viscosity, kg m^{-1} s^{-1}
ρ density, kg m^{-3}
φ volume fraction occupied by the internal duct, dimensionless

Subscripts

ds dry solid
eff effective
f fluid
g glass
in inlet
m minimized
max maximum
opt optimal
r, z velocity vector components
s solid
0 initial
∞ environmental condition

7. REFERENCES

1. G. Viccini, D. A. Mitchell, S. D. Boit, J. C. Gern, A. S. Rosa, R. M. Costa, F. D. H. Dalsenter, O. F. von Meien and N. Krieger, Analysis of growth kinetic profiles in solid state fermentation, *Food Technol. Biotechnol.*, vol. 39, pp. 271-294, 2001.
2. A. Pandey, C. R. Soccol and D. Mitchell, New developments in solid state fermentation: I-bioprocesses and products, *Process Biochem.*, vol. 35, pp. 1153-1169, 2000.
3. Y. S. P. Rahardjo, J. Tramper and A. Rinzema, Modeling conversion and transport phenomena in solid-state fermentation: A review and perspectives, *Biotechnol. Adv.*, vol. 24, pp. 161-179, 2006.
4. Z. Hamidi-Esfahani, S. A. Shojaosadati and A. Rinzema, Modelling of simultaneous effect of moisture and temperature on A. niger growth in solid-state fermentation, *Biochem. Eng. J.*, vol. 21, pp. 265-272, 2004.
5. U. Hölker, M. Höfer and J. Lenz, Biotechnological advantages of laboratory-scale solid-state fermentation with fungi, *Appl. Microbiol. Biotechnol.*, vol. 64, pp. 175-186, 2004.
6. M. Raimbault, General and microbiological aspects of solid substrate fermentation, *Electron. J. Biotechnol.*, vol. 1 (3), pp. 174-188, 1998.
7. S. R. Couto and M. A. Sanromán, Application of solid-state fermentation to food industry - A review, *J. Food Eng.*, vol. 76 (3), pp. 291-302, 2006.
8. H. Z. Chen, J. Xu and Z. H. Li, Temperature control at different bed depths in a novel solid-state fermentation system with two dynamic changes of air, *Biochem. Eng. J.*, vol. 23, pp. 117-122, 2005.
9. F. D. H. Dalsenter, G. Viccini, M. C. Barga, D. A. Mitchell and N. Krieger, A mathematical model describing the effect of temperature variations on the kinetics of microbial growth in solid-state culture, *Process Biochem.*, vol. 40 (2), pp. 801-807, 2005.
10. A. Bejan, Constructal-theory network of conducting paths for cooling a heat generating volume, *Int. J. Heat Mass Transfer*, vol. 40, pp. 799-816, 1997.
11. A. Bejan, *Shape and Structure, from Engineering to Nature*, Cambridge University Press, Cambridge, UK, 2000.
12. L. A. O. Rocha, E. Lorenzini and C. Biserni, Geometric optimization of shapes on the basis of Bejan's Constructal Theory, *Int. Commun. Heat Mass Transfer*, vol. 32 (10), pp. 1281-1288, 2005.
13. L. A. O. Rocha, S. Lorente and A.Bejan, Conduction tree networks with loops for cooling a heat generating volume, *Int. J. Heat Mass Transfer*, vol. 49 (15-16), pp. 2626-2635, 2006.
14. C. Biserni, L. A. O. Rocha, G. Stanescu and E. Lorenzini, Constructal H-shaped cavities according to Bejan's theory, *Int. J. Heat Mass Transfer*, vol. 50, pp. 2132-2138, 2007.
15. H. Wang, W. Dai and A. Bejan, Optimal temperature distribution in a 3D triple-layered skin structure embedded with artery and vein vasculature and induced by electromagnetic radiation, *Int. J. Heat Mass Transfer*, vol. 50, pp. 1843-1854, 2007.
16. D. Mitchell, R. Parra, D. Aldred and N. Magan, Water and temperature relations of growth and ochratoxin A production by *Aspergillus carbonarius* strains from grapes in Europe and Israel, *J. Appl. Microb.*, vol. 97, pp. 439-445, 2004.
17. R. Parra, D. Aldred, D. B. Archer and N. Magan, Water activity, solute and temperature modify growth and spore production of wild type and genetically engineered *Aspergillus niger* strains, *Enzyme Microb. Technol.*, vol. 35, pp. 232-237, 2004.

18. S. D. M. Hasan, Modelagem e simulação da transferência de calor em fermentação semi-sólida de farelo de arroz, Master's Dissertation, Federal University of Rio Grande, RS, Brasil, 1998.
19. P. Sangsurasak and D. A. Mitchell, Validation of a model describing two-dimensional heat transfer during solid-state fermentation in packed bed bioreactors, *Biotechnol. Bioeng.*, vol. 60 (6), pp. 739-749, 1998.
20. D. A. Mitchell, A. Pandey, P. Sangsurasak and N. Krieger, Scale-up strategies for packed-bed bioreactors for solid-state fermentation, *Process Biochem.*, vol. 35, pp. 167-178, 1999.
21. V. M. Ashley, D. A. Mitchell and T. Howes, Evaluating strategies for overcoming overheating problems during solid-state fermentation in packed bed bioreactors, *Biochem. Eng. J.*, vol. 3, pp. 141-150, 1999.
22 D. A. Mitchell, O. F. von Meien and N. Krieger, Recent developments in modeling of solid-state fermentation: heat and mass transfer in bioreactors, *Biochem. Eng. J.*, vol. 13 (2-3), pp. 137-147, 2003.
23. F. J. Weber, J. Oostra, J. Tramper and A. Rinzema, Validation of a model for process development and scale-up of a packed-bed solid-state bioreactors, *Biotechnol. Bioeng.*, vol. 77 (4), pp. 381-393, 2002.
24. G. Saucedo-Castañeda, M. Gutiérrez-Rojas, G. Bacquet, M. Raimbault, G. Viniegra-González, Heat transfer simulation in solid substrate fermentation, *Biotechnol. Bioeng.*, vol. 35, pp. 802-808, 1990.
25. J. A. V. Costa, R. M. Alegre and S. D. M. Hasan, Packing density and thermal conductivity determination for rice bran solid-state fermentation, *Biotechnol. Tech.*, vol. 12 (10), pp. 747-750, 1998.
26. A. Bejan, *Convection Heat Transfer*, Wiley, New York, 2004.
27. P. Sangsurasak and D. A. Mitchell, The investigation of transient multidimensional heat transfer in solid state fermentation, *Chem. Eng. J.*, vol. 60, pp. 199-204, 1995.
28. P. Sangsurasak and D. A. Mitchell, Incorporation of death kinetics into a 2-dimensional dynamic heat transfer model for solid state fermentation, *J. Chem. Technol. Biotechnol.*, vol. 64, pp. 253-260, 1995.
29. S. D. M. Hasan, J. A. V. Costa and A. V. L. Sanzo, Heat transfer simulation of solid state fermentation in packed-bed bioreactor, *Biotechnol. Tech.*, vol. 12 (10), pp. 787-791, 1998.
30. T. L. Richard, A. H. M. Veeken, V. de Wilde and H. V. M. Hamelers, Air-filled porosity and permeability relationships during solid-state fermentation, *Biotechnol. Progr.*, vol. 20, pp. 1372-1381, 2004.
31. P. E. Liley, G. H. Thomson, D. G. Friend, T. E. Daubert and E. Buck, Physical and Chemical Data, in: R. H. Perry, D. W. Green and J. O. Maloney (Eds.), *Perry´s Chemical Engineers´ Handbook*, MacGraw-Hill, New York, 1999.
32. N. P. Ghildyal, M. K. Gowthaman, K. S. M. S. Raghava Rao and N. G. Karanth, Interaction of transport resistances with biochemical reaction in packed-bed solid-state fermentor: Effect of temperature gradients, *Enzyme Microb. Technol.*, vol. 16, pp. 253-257, 1994.
33. D. A. Mitchell, O. F. von Meien, N. Krieger and F. D. H. Dalsenter, A review of recent developments in modeling of microbial growth kinetics and intraparticle phenomena in solid-state fermentation, *Biochem. Eng. J.* , vol. 17, pp. 15-26, 2004.
34. B. Barros Neto, I. S. Scarminio and R. E. Bruns, Como fazer experimentos: pesquisa e desenvolvimento na ciência e na indústria, Editora da Unicamp, Campinas, BR, 2003.
35. V. G. Martins, S. J. Kalil, T. E. Bertolin and J. A. V. Costa, Solid state biosurfactant production in a fixed-bed column bioreactor, *Z. Naturforsch. C J. Biosci.*, vol. 61 (9-10), pp. 721-726, 2006.